Supplementary Material for:

Backwater controls on avulsion location on deltas

Phairot Chatanantavet[1], Michael P. Lamb[1], and Jeffrey A. Nittrouer[2]

Geophysical Research Letters, 2012, v. 39

[1]*Division of Geological and Planetary Sciences, California Institute of Technology, Pasadena, CA 91125*

[2]*Department of Geology, University of Illinois at Urbana-Champaign, Urbana, IL 61801*

Supplementary Materials

In this supplementary material file we provide 1) an image of the Mississippi River during flood showing the turbid river plume (Figure S1), 2) methods for estimating the backwater length scale for natural rivers (Section S1), 3) database of deltaic river characteristics used in Figure 1D (Table S1), and 4) the governing equations and calculation procedure (Section S2).

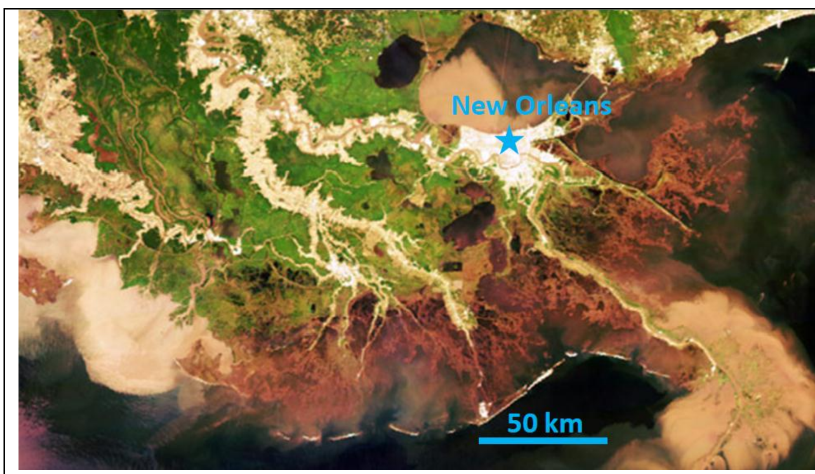

Figure S1. Sediment-laden plume during the great flood of 2011 in the Mississippi River. Source: NASA Aqua Satellite.

S1. Method to Calculate Backwater Length for Field Cases

We calculated the backwater length (L_b) for nine rivers (Fig. 1) following [e.g. *Parker*, 2004]:

$$L_b \sim h_c/S \tag{S1}$$

$$h_c = \left(\frac{C_f Q_c^2}{g w^2 S}\right)^{1/3} \tag{S2}$$

where h_c is the characteristic flow depth, S is the bed slope, C_f is a bed friction coefficient, Q_c is a characteristic water discharge, w is channel width and g is gravitational acceleration. We quantified the characteristic discharge by calculating the peak annual flood event with a two-year recurrence interval [e.g., *Wilkerson*, 2008] from recorded flow data from the Oak Ridge National Laboratory Distributed Active Archive Center and the U.S. Army Corps (Table S1). The channel slope for each river was calculated from existing literature [*Depetris and Gaiero*, 1998; *Saad*, 2002; *Giosan et al*., 2005; *Jerolmack and Mohrig*, 2007; *Lamb et al*., in press]. Channel width was measured from satellite images. The friction coefficient was assumed to be equal to 0.002 for all cases, which is a typical value for large lowland rivers [*Parker et al*., 2007]. The upstream distance from the river mouth to the avulsion node, L_A, was measured along the river centerline from satellite imagery (Fig. 1).

Table S1. Database of deltaic river characteristics.

River	Width (m)	Slope	Q_c (m^3/s)	h_c (m)	L_b (km)	L_a (km)
Parana River	1,270	0.00004	22,800	11.8	295	210
Danube River	1,250	0.00005	9,700	6.3	125	95
Nile River, Egypt	240	0.000064	8,800	16.2	254	210
Lower Mississippi River, USA	650	0.000043	29,000	21.0	480	490
Assiniboine R., Manitoba	100	0.0005	1,350	4.2	8.4	12
Rhine-Meuse River	700	0.00011	5,750	5.0	45.5	51
Magdalena R. Colombia	1,100	0.000095	11,040	6.0	63.2	67
Orinoco R. Venezuela	2,000	0.00006	24,550	8.0	133.3	78
Mid Amazon (@Negro R.)	3,000	0.00003	47,800	12.0	400	404

S2. Governing Equations and Model Procedure

Conservation of fluid mass and momentum of the depth-averaged and width-averaged, 1-D spatially varied flow in the streamwise (x) direction [e.g., *Chow*, 1959] can be written as:

$$\frac{d(Uhw)}{dx} = 0 \quad \text{(S3)}$$

$$U\frac{dU}{dx} = -g\frac{dh}{dx} + gS - C_f\frac{U^2}{h} \quad \text{(S4)}$$

where U is the depth-averaged streamwise flow velocity and h is flow depth. The combination of equations (S3) and (S4) leads to a standard formulation of the backwater equation for spatially varied flow [*Chow*, 1959],

$$\frac{dh}{dx} = \frac{S + Fr^2\left(\frac{h}{w}\frac{dw}{dx} - C_f\right)}{1 - Fr^2} \quad \text{(S5)}$$

where $Fr = U/\sqrt{gh}$ is Froude number.

Offshore, river plumes tend to spread laterally and sometimes vertically due to loss of river-channel confinement resulting in offshore deposition and a water surface elevation at the river mouth is relatively insensitive to changes in river discharge as compared to farther upstream [e.g., *Rajaratnam*, 1976; *Wright*, 1977; *Rowland et al.*, 2009; *Schiller and Kourafalou*, 2010]. For example, stage height increases by < 1 m at the mouth of the Mississippi River during large floods, whereas stage heights can increase by > 10 m farther upstream [e.g., *Karadogan et al.*, 2009]. The simplest way to incorporate the effect of lateral plume spreading would be to force the water surface elevation at the river mouth to be at sea level through use of a boundary condition at $x = 0$ in equation (S5) [e.g., *Parker et al.*, 2008; *Karadogan et al.*, 2009]. We have found, however, that forcing the water surface to sea level at $x = 0$ is too restrictive and can produce a drawdown effect that is greater than observed [*Lamb et al.*, in press]. To allow for some variation of the water-surface elevation at the river mouth, we instead treat the offshore plume as a depth-averaged, steady, homopycnal current, where momentum is balanced in 1-D between a hydrostatic pressure gradient and drag along the bed (i.e., equation (S5)). We neglect drag and entrainment along the lateral margins of the plume and represent lateral spreading of the plume geometrically by assigning a set spreading angle (θ) beyond the shoreline ($x < 0$). Thus, in equation (S5), the average width of the plume beyond the shoreline (i.e., $x < 0$) is calculated from $\frac{dw}{dx} = 2\tan\theta$ where θ is the spreading angle of the plume relative to the center streamline. Theory, experiments, and field observations have found that unconfined jets tend to spread at an angle of ~ 5.7 degrees when width-averaged [e.g., *Wright and Coleman*, 1971; *Rajaratnam*, 1976; *Wang*, 1984; *Rowland et al.*, 2010], which we employ here. Although our representation of the plume is highly simplified, it is sufficient to reproduce the desired effect of a dynamic river-mouth, water-surface elevation that is a model outcome (rather than a boundary condition).

To solve equation (S5), the bed elevation, bed slope, channel width and discharge are specified everywhere along the flow path. For subcritical flow ($Fr < 1$) considered here, the water level in the basin is fixed at sea level very far downstream of the region of interest ($x << 0$), which allows a dynamic water-surface elevation at the shoreline. The calculation for flow depth proceeds in an upstream direction from this boundary condition.

We use *Engelund and Hansen* [1967] for calculating transport rate of total bed-material load (Q_s),

$$Q_s = w(RgD_{50}^3)^{1/2}\left(\frac{0.05}{C_f}\right)\tau_*^{5/2} \tag{S6}$$

where R is the submerged specific density of the sediment (~ 1.65), D_{50} is the median grain size, $\tau_* = u_*^2/RgD_{50}$ is the Shields stress, and $u_* = \sqrt{C_f U^2}$ is the shear velocity. The evolution of the bed by continuity for dilute flow can be written as

$$(1-\lambda_p)\left(\frac{\partial \eta}{\partial t} + \sigma\right) = -\frac{1}{w_s}\frac{\partial Q_s}{\partial x} \tag{S7}$$

where λ_p is bed porosity. σ is the rate of relative sea-level rise (i.e., subsidence rate plus eustatic sea-level rise), which we treat as uniform; however, in cases subsidence may be spatially variable (e.g., Mississippi River [*Blum and Roberts*, 2009]). w_s is the width of the depositional zone. In the river ($x > 0$), the width of the depositional zone is equivalent to the channel width (i.e., $w_s = w$). The offshore depositional zone, however, can span a much larger area than the width of the river plume itself over geomorphic timescales because of variability in the plume location, bifurcations, and waves, tides, and other processes that tend to distribute sediment away from the river mouth. To account for these effects using our quasi-2D framework, we follow previous work [e.g., *Parker and Sequeiros*, 2006; *Kim et al.*, 2009] and set the effective width of the offshore (i.e., $x < 0$) depositional zone to $w_s = w_o + 2x\tan\theta_s$, where w_o is the river channel width and the deposit spreading angle, $\theta_s = 70^o$. This deposit spreading angle was approximated from satellite images of the Mississippi River Delta (e.g., Fig. S1). Greater spreading angles result in slower delta growth, but do not significantly affect our predictions of the avulsion lengthscale.

Equations (S5) – (S7) represent the river-plume model, which links hydrodynamics, sediment transport, and bed morphology and simulates the interactions among them. For the model case of the Mississippi River, we set the initial channel bed slope to $S = 4 \times 10^{-5}$, channel width to $w_o = 650$ m, bed friction coefficient $C_f = 0.002$, median grain diameter to $D_{50} = 300$ μm [*Thorne et al.*, 2008], bed porosity to $\lambda_p = 0.40$, and the initial water depth at the shoreline to 25 m. Note that simulated erosion rates may overestimate modern rates in parts of the lower 200 km of the Mississippi River, which show degradation into consolidated alluvium [*Nittrouer et al.*, 2011].

To run the variable discharge simulation, daily water discharge data from U.S. Army Corps were linearly split into six bins with average discharges of 6.2×10^3, 1.2×10^4, 1.9×10^4, 2.6×10^4, 3.2×10^4, and 3.9×10^4 m^3/s and corresponding fractional time of occurrence of 0.36, 0.28, 0.19, 0.12, 0.04, and 0.01. We solved the governing equations using finite difference approximations (first-order in time with a time-step of 0.05 yrs. and second-order in space with a spatial step of 12 km) for a complete cycle of the six discharges (from lowest to highest discharge) for a period of 30 years, which corresponds to the peak-annual-flood recurrence interval of the largest flood event considered. This cycle was repeated to reach $T_A = 1500$ years of total run time.

The model predictions of sediment flux in the fluvial section are in agreement with those measured by the U.S. Geological Survey during both low flows and high flows at St. Francisville station (x = 425 km) [*Nittrouer et al.*, in press]; for example, Q_s= 0.2 m^3/s for Q_w = 12,000 m^3/s and Q_s = 1 m^3/s for Q_w = 39,000 m^3/s. A detailed comparison of model hydrodynamic predictions and historic observations for the case of the Mississippi River can be found in *Lamb et al.* [in press].

In our simulations we have neglected overbank flow over an extensive floodplain. This is a reasonable assumption for the Mississippi River, as the levees are capable of containing most high discharge events up to ~ Q_w = 4 x 10^4 m^3/s, which is well within the drawdown regime [*Lamb et al.*, in press]. The effect of a coupled floodplain on drawdown dynamics likely depends on the nature of floods in a particular river system. For example, flow from the channel to the floodplain would reduce the rate of water-surface elevation rise in the channel, which in turn could reduce the magnitude of drawdown during high flows, potentially making our predicted avulsion location metrics less pronounced, at least until the floodplain is fully inundated. However, in some rivers (including reaches of the Mississippi), water levels can rise contemporaneously in the floodplain and channel, or water can flow from the floodplain to the channel due to floodplain inundation from upstream sources or direct precipitation [e.g., *Mertes*, 1997; *Day et al.*, 2008]. In these cases, the floodplain may have little effect on the preferential avulsion zone.

S3. References

Blum, M.D. and H.H. Roberts (2009), Drowning of the Mississippi Delta due to insufficient sediment supply and global sea-level rise, *Nature Geosci*., 2, 488-491, doi:10.1038/ngeo553

Chow, V. T. (1959), *Open Channel Hydraulics*, 680 pp., McGraw Hill.

Day, G., W. E. Dietrich, J. C. Rowland, and A. Marshall (2008), The depositional web on the floodplain of the Fly River, Papua New Guinea, *J. Geophys. Res*., 113, F01S02, doi:10.1029/2006JF000622

Depetris, P.J. and D.M. Gaiero (1998), Water-Surface Slope, Total Suspended Sedimentand Particulate Organic Carbon Variability in the Parana River During Extreme Flooding, Short Communications, Naturwissenschaften, Springer-Verlag, 85, 26–28.

Engelund, F., and E. Hansen (1967), *A monograph on sediment transport in alluvial streams*, Copenhagen.

Giosan, L., J. P. Donnelly, E. Vespremeanu, J.P., Bhattacharya, C. Olariu, F.S. Buonaiuto (2005), River delta morphodynamics: examples from the Danube Delta, *River Deltas—Concepts, Models, and Examples*, SEPM Special Publication No. 83, ISBN 1-56576-113-8, p. 393–411.

Jerolmack, D. J., and D. Mohrig (2007), Supplemental material (including references for data base therein) - Conditions for branching in depositional rivers, *Geology*, 35(5), 463-466., doi: 10.1130/G23308A.1

Karadogan, E., C. S. Willson, and C. R. Berger (2009), Numerical modeling of the Lower Mississippi River-influence of forcings on flow distribution and impact of sea level rise on the system, in OCEANS 2009, MTS/IEEE Biloxi - Marine Technology for Our Future: Global and Local Challenges, 1-7.

Kim, W., A. Dai, T. Muto, and G. Parker (2009), Delta progradation driven by an advancing sediment source: Coupled theory and experiment describing the evolution of elongated deltas, *Water Resour. Res*., W06428, 45, doi:10.1029/2008WR007382.

Lamb, M. P., J.A. Nittrouer, D. Mohrig, and J. Shaw (in press), Backwater and river-plume controls on scour upstream of river mouths: Implications for fluvio-deltaic morphodynamics, *J. Geophys. Res.-Earth Surf. doi: 10.1029/2011JF002079.*

Mertes, L. A. K. (2002), Remote sensing of riverine landscapes*, Freshw. Biol*., 47(4), 799-816.

Nittrouer, J. A., D. Mohrig, M. A. Allison, and A.P.B Peyret (2011), The Lowermost Mississippi River: A mixed bedrock-alluvial channel, *Sedimentology*, DOI: 10.1111/j.1365-3091.2011.01245.x.

Nittrouer, J.A., Shaw, J., Lamb, M.P., Mohrig, D. (in press), Spatial and temporal trends for water-flow velocity and bed-material transport in the lower Mississippi River. *Geol. Soc. of Amer. Bull*.

Oak Ridge National Laboratory Distributed Active Archive Center, records of water discharge for world rivers, http://daac.ornl.gov/rivdis/STATIONS.HTM#A

Opreanu, G. (2010), Identifying erosion areas along the Danube on the basis of grain-size and hydrologic parameters, *Geo-Eco-Marina*, 16, p. 101-106.

Parker, G. (2004), 1-D sediment transport morphodynamics with applications to rivers and turbidity currents, e-book., http://vtchl.uiuc.edu/people/parkerg/morphodynamics_e-book.htm

Parker, G., T. Muto, Y. Akamatsu, W.E. Dietrich, and J.W. Lauer (2008), Unravelling the conundrum of river response to rising sea-level from laboratory to field. Part I: Laboratory experiments, *Sedimentology*, *55*(6), 1643-1655, DOI: 10.1111/j.1365-3091.2008.00961.x

Parker, G. and O. Sequeiros (2006), Large scale river morphodynamics: application to the Mississippi Delta, River flow 2006 Conference, Lisbon, Portugal, Proceedings of the International Conference on Fluvial Hydraulics, edited by R. M. L. Ferreira et al., pp. 3–11, Taylor and Francis, London.

Parker, G., P.R. Wilcock, C. Paola, W.E. Dietrich, and J. Pitlick (2007), Physical basis for quasi-universal relations describing bankfull hydraulic geometry of single-thread gravel bed rivers, *J. Geophys. Res. – Earth Surf.*, 112, F04005, 21 pp., doi:10.1029/2006JF000549

Rajaratnam, N. (1976), *Turbulent Jets*, Elsevier., New York, 302 pp.

Rowland, J. C., W.E. Dietrich, and M.T. Stacey (2010), Morphodynamics of subaqueous levee formation: Insights into river mouth morphologies arising from experiments, *J. Geophys. Res.-Earth Surf.*, *115*, F04007, 20 pp., doi:10.1029/2010JF001684

Rowland, J.C., M.T. Stacey, and W.E. Dietrich (2009), Turbulent characteristics of a shallow wall-bounded plane jet: experimental implications for river mouth hydrodynamics, *J. Fluid Mech*., 627, 423-449, DOI: 10.1017/S0022112009006107

Saad, M.B.A. (2002), Nile River morphology changes due to the construction of high Aswan dam in Egypt, Ministry of Water Resources and Irrigation Report, Egypt, 14 pages.

Schiller, R. V., and V. H. Kourafalou (2010), Modeling river plume dynamics with the HYbrid Coordinate Ocean Model, *Ocean Model.*, *33*(1-2), 101-117.

Thorne, C., O. Harmar, C. Watson, N. Clifford, D. Biedenharn, and R. Measures (2008), Current and historical sediment loads in the lower Mississippi River, Report to United States Army, European research office of the U.S. ARMY, University of Nottingham, U.K., 220 pp.

Wang, F. C. (1984), The dynamics of a river-bay-delta system, *J. Geophys. Res.*, 89(NC5), 8054-8060, doi: 10.1029/JC089iC05p08054

Wilkerson, G.V. (2008), Improved bankfull discharge prediction using 2-year recurrence-period discharge, *J. of the Amer. Water Resour. Asso*., 44(1), 243-257, DOI: 10.1111/j.1752-1688.2007.00151.x

Wright, L. D.(1977), Sediment transport and deposition at river mouths: A synthesis, *Geological Society of America Bulletin*, 88(6), 857-868.

Wright, L.D. and J.M. Coleman (1971), Effluent expansion and interfacial mixing in the presence of a salt wedge, Mississippi River delta, *J. Geophys. Res*., 76(36), 8649-8661, doi: 10.1029/JC076i036p08649.

Wright, S., and G. Parker (2004), Flow resistance and suspended load in sand-bed rivers: Simplified stratification model, J. of Hydraulic Eng., 130(8), 796-805, doi: 10.1061/(asce)0733-9429(2004)130:8(796).